Document Discussion

Return To Library > Records > ERID-98500 through ERID-99000 > ERID-098533 1) VAPOR-PHASE TRANSPORT BENEATH MDA L- DRUM FAILURE SIMULATION WITH IMPLICATIONS FOR SITE REMEDIATION

Created By:	Nicole M. Valerio/USERS/LANL
File name:	Target-ERID # for Domino.txt
Version:	1.0
Document Type:	RPF Record
Description:	RECORD SUBMITTED BY: RACHEL COWAN
	REFERENCE CITED

Document Details:

Title:	ERID-098533 1) VAPOR-PHASE TRANSPORT BENEATH MDA L- DRUM FAILURE SIMULATION WITH IMPLICATIONS FOR SITE REMEDIATION
ERID Number.StartPage:	ERID-098533
Office of Record:	ENV-ERSS
Date Received:	10/10/2007
Official Use Only:	N
Page Count:	27
Record Type:	Report
Document Date:	04/01/2007
To:(Addressees - Organization) *(separate multiple values with semicolons)*	N/A
From:(Senders - Organization) *(separate multiple values with semicolons)*	PHILIP H. STAUFFER JOHN K. HOPKINS
Other Document Number(s): *(separate multiple values with semicolons)*	N/A
TA: *separate multiple values with semicolons)*	N/A
PRS Number(s): *(separate multiple values with semicolons)*	N/A
Record Box Number:	

*** Denotes Fields that are mandatory.**

To download this file, right mouse click on the file and select 'Save to Disk' or 'Save Target as'

Target-ERID # for Domino.txt <-- This link points to this version.

To check-out and/or edit this file, select Edit Document or Check Out Document from the Document menu above.

File Cabinet: Records

Binder Category: ERID-90000 through ERID-99999

30960

rfp - records@LANL.gov

LANL Environmental Records Transmittal Form

Instructions: This form must be completed and submitted with all individual records or record packages by the record originator.

Transmittal Date: 5 Oct 0~~5~~7 **Official Use Only:** Yes No **UCNI:** Yes No **Page 1 of** 2

Transmitter Information: Z#: 224287 Name: Rachel Cowan E-Mail: cowanr@p2S.com Transmitter Org.: Pro 2 Serve

Contamination Potential: To the best of my knowledge, the records(s) have no radioactive contamination. **Signature:** Rachel Cowan

Record Type: Individual Records (No Package) New Package Existing Package (Add) Resubmit/Supersedes Record#: _____

Package #(s): _____ Package Title(s): _____

Reference/Retrieval Information:

Organization/Program: ERSS Project: MDA G CME Plan Revision 2 & Response to NOD TA(s): 54

Record (Package) Contents

Record Title (Limited to 255 characters)	Media Type	Doc. Date	Author/ Originator	Other Doc. Numbers (LAUR, DocCatalog#, Symbol or N/A)	Page Count	ERID# (RPF Only)
~~Groundwater Pathway Model for the Los Alamos National Laboratory Technical Area 54, Material Disposal Area G~~		~~Sept. 2005~~	~~P. Stauffer, H. Viswanathan, B. Robinson, C. Gable, G. Cole, D. Broxton, E Springer & T Schofield~~	~~LA-UR-05-7393~~	~~65~~	~~097432~~
Vapor-Phase Transport Beneath MDA-L: Drum Failure Simulations w/ Implications for Site Remediation		April 2004	Phillip H. Stauffer & John K. Hopkins		27	098033

(Use additional continuation forms as needed)

Records Processing Facility Use Only: (Names & Dates)
Accepted: N 10/10/07 **Entered:** N 10/10/07 **Scanned:** mr 12/13/07 **QC:** mr 12/13/07

098533
27

Vapor-Phase Transport Beneath MDA-L:

Drum Failure Simulations with Implications for Site Remediation

Philip H. Stauffer[1]

John K. Hopkins[2]

1) EES-6, Earth and Environmental Sciences Division

2) ECR, Risk Reduction and Environmental Stewardship Division

Los Alamos National Laboratory

Los Alamos NM, 87545

April 2004

RECEIVED
OCT 10 2007
By

1.0 - Abstract

This paper is a continuation of a previous paper in which a numerical model was created and used to calibrate a best-fit simulation of subsurface vapor-phase transport of trichloroethane (TCA) using a set of 132 borehole vapor measurements of volatile organic compounds (VOCs) made at the former Los Alamos National Laboratories liquid waste disposal area, MDA L. The simulations use a finite volume heat and mass transport code that solves the diffusion equation and includes Henry's Law partitioning between the liquid and vapor phases. The calculations are performed on a numerical grid that incorporates local topography and honors existing knowledge of subsurface geology in three dimensions. The best-fit simulation was run from 1975 until the year 2000 and had a year 2000 model/data correlation of 1.03, where 1.00 is a perfect match between model and data. The conceptual model for source release in the best-fit simulation is slow leaking of TCA vapor leading to relatively constant source region TCA concentrations in the range of 3000 ppmv, well below the saturated vapor pressure of 160,000 ppmv that would be seen when TCA vapor is in equilibrium with a liquid source.

In this paper, the best-fit model is used to examine the probable effects of barrels failing in the subsurface and creating a sudden impulse of VOC to the system. Liquid transport is not specifically computed, however the VOC source region is located beneath the waste shafts from approximately 60 ft to 140 ft deep and is meant to represent possible liquid flow to these depths prior to volatilization. Additionally, the sudden release scenario allows the partial pressure of TCA to reach its saturated vapor pressure (160,000 ppmv). The model is used to determine the signal that a drum failure would cause at several monitoring boreholes situated around the source region. The simulations show that for a small number of barrel failures (less than five), the increase in pore-gas concentrations above the expected plume growth is relatively small and would be detected conclusively only in boreholes quite near the region of failure. For a large number of drum failures (ten or more), the expected increase in concentration above the background plume is quite large and could be seen in several of the boreholes surrounding the site. Additionally, in the absence of a vapor extraction system, simultaneous release of twenty five 55-gallon drums (7000 kg) of TCA would lead to a significant increase in the plume depth and concentrations. The results of this modeling study will be used to support the development of a long-term monitoring plan and aid in the design of a vapor extraction system to control possible future plume growth.

2.0 - Introduction

The purpose of this work is to use a calibrated numerical model of the vadose zone VOC plume at MDA L (Stauffer et al., 2004) to examine the possible effects of catastrophic failure of 55-gallon drums containing volatile liquid waste. Although drum failure in the arid subsurface is poorly understood, attempts have been made to characterize the distribution of such failure for painted stainless-steel drums under earthen covers (Lyon et al., 1996). Lyons et al. (1996) present useful data from drums stored at Los Alamos under conditions that may be similar to those found in the shafts at MDA L. The Lyons study suggests that the drums of VOC found at MDA L will corrode slowly over the next hundred years at a rate of between 0.5 to 4 mil/year (mil = 1/1000 inch).

Lyons et al. (1996) recognize two styles of corrosion, general corrosion and pitting corrosion. These two styles of corrosion lead to quite different types of failures. General failure causes an overall loss of structural integrity of the drum when the wall thickness is reduced to less than 10 mils, and we will refer to this mechanism as catastrophic failure for the rest of the paper. Pitting failure causes tiny holes that breach the drum at the point of failure, while the structural integrity is still intact (Lyons et al., 1996). The results of Lyons et al.(1996), for a typical corrosion rate of 1 mil/year, imply that for steel drums of 55 mil thickness, most probable time to general failure is on the order of 45 years. The probabilistic nature of their model leads to a distribution around the mean failure time beginning at about 30 years with failure of most drums predicted by 70 years.

The scope of this paper is limited to calculations of the short-term effects (30 years) of catastrophic drum failure on pore-gas concentrations at nearby monitoring points. By examining a range of possible scenarios and their consequences, this work highlights continued uncertainty in parameters associated with waste emplacement such as the total volume of waste, the total number of barrels, the percent of barrels containing adsorbent material, the type of waste containers, and the distribution and style of container failures that one should expect in the future. The calibrated model is shown to be a useful tool for understanding the behavior of this waste site under a variety of conditions. The results will be used for development of a consistent and logical approach for monitoring and remediation for the lifetime of this waste site, including analysis of how venting technology may be used to reduce the long term plume growth predicted from either slow leaking through pinholes or the higher impact plume growth caused by catastrophic general failure of

multiple drums. Additionally, the model can be used to study changes in the site, such as removal of the asphalt upon closure and installation of a landfill cover.

3.0 - Site description

Located on a Mesita del Buey within the boundaries of Los Alamos National Laboratory, Material Disposal Area L (MDA L) was the Laboratory's subsurface liquid, chemical-waste disposal facility that operated from the late 1950's through 1986 [LANL, 2000]. The major chemicals of potential concern (COPC) measured at this site are VOCs [LANL, 2000]. After passage of the Resource Conservation and Recovery Act (RCRA), regulations concerning the disposal and storage of hazardous waste caused the Laboratory to discontinue subsurface disposal of RCRA regulated chemical wastes.

3.1 Stratigraphy and topography

The strata that immediately underlie MDA L are composed of nonwelded to moderately welded rhyolitic ash-flow and ash-fall tuffs interbedded with thin pumice beds. The canyons on either side of MDA L, Canada del Buey and Pajarito Canyon, lie approximately 30 m below the steep-sided mesa (Figure 1). Figure 2 shows a simplified stratigraphic column of the rocks underlying MDA L. More discussion of the site geology can be found in Reneau et al. (1998) and Vaniman et al. (1998).

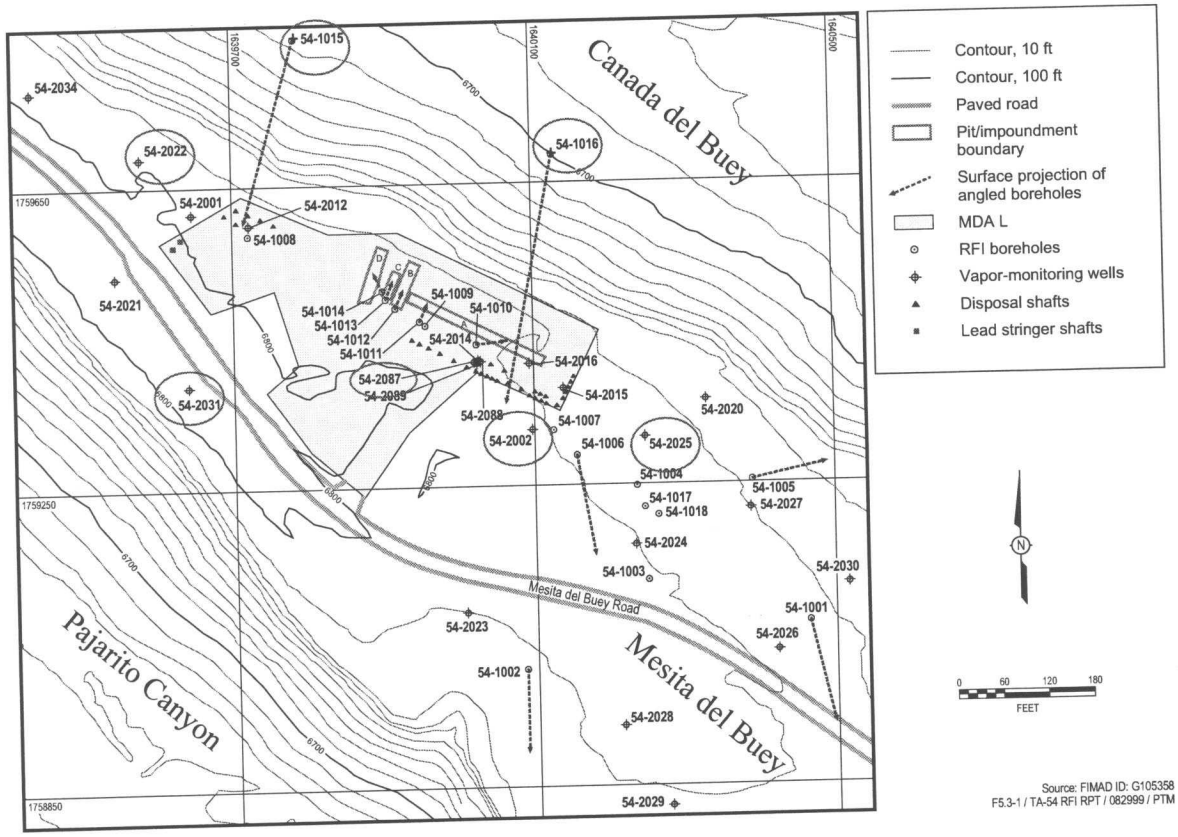

Figure 1 Geographical information for MDA L and the surrounding area. Boreholes used in this study to monitor expected differences in pore-gas concentration are highlighted with open red circles.

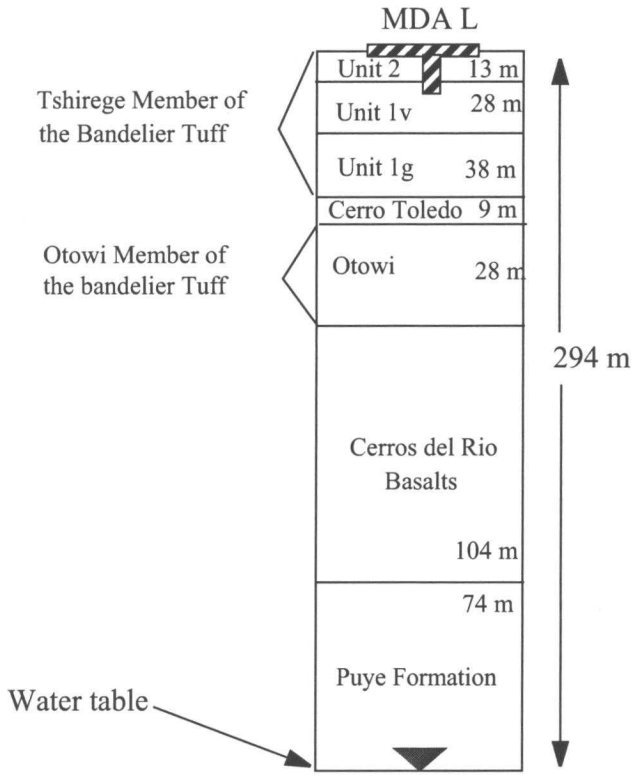

Figure 2 Simplified site stratigraphy.

3.2 Contaminant source

3.2.1 Timing of waste disposal at MDA L

Thirty four disposal shafts containing drums of liquid waste are considered for this study as the Potential Release Sites (PRS) at MDA L (Figure 3) [LANL, 2000]. Operation dates for the 34 disposal shafts ranged from 1975 to 1985. Shaft numbers 1 through 28 operated from 1975 through 1985, while shaft numbers 29 through 34 operated from 1983 through 1985. After decommissioning, most of the 2.5 acres comprising MDA L were covered with asphalt upon which were built temporary storage facilities for hazardous waste.

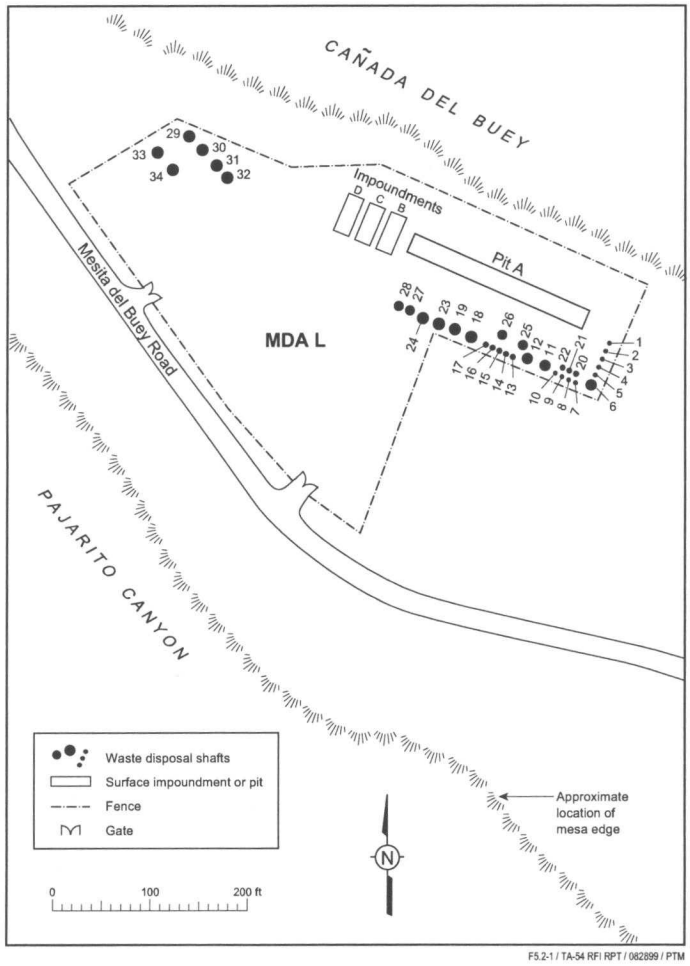

Figure 3 Location map for waste disposal shafts and pits at MDA L

3.2.2 VOC sources at MDA L

There is little information on specific chemicals, timing, or quantities of waste that were disposed of at MDA L. However, the major COPCs measured at this site are found in pore-gas sampling and contain a host of VOCs [LANL, 2000].

The 34 shafts received 55-gallon steel drums (approximately 200 liters) containing chemical liquid waste. The waste drums were packed in lifts with one to six barrels per layer. In the shafts, layered waste was covered with crushed tuff to provide absorbent material as well as structural support for the drums. Additionally, unknown quantities of small containers and free product were dropped directly into the shafts. The locations of the pits and shafts can be seen in Figure 3. Records indicate that the majority of material placed in the shafts was organic waste. The records do not differentiate between pure liquid and organic contaminated solids (rags, paper, etc.). However, because MDA L was a designated liquid waste disposal area, contaminated solids were most likely disposed of at other LANL MDAs. Although we cannot rule out the possibility that free

product existed at some point in time, no free product was found in any of the boreholes drilled at the site. Furthermore, at an average mesa top pressure of approximately 800 mb, the vapor pressure of 1,1,1-TCA (13.1 kPa Table 1) would lead to vapor concentrations of over 160,000 ppmv. Because measured concentrations are more than an order of magnitude below the 1,1,1-TCA vapor-liquid equilibrium concentration, the vapor monitoring data provide an additional strong line of evidence that free product (i.e. liquid) is not currently present in significant quantities. For comparison, gasoline at 20C has a vapor pressure of approximately 28 kPa (350,000 ppmv at liquid vapor equilibrium). Thus gasoline and TCA behave in a similar manner with respect to evaporation and it is expected that any liquid TCA should evaporate quickly. Mixtures of liquids will result in the vapor pressure of a given constituent being reduced by the molar ratio of that constituent in the liquid (Fetter, 1999), however at this site TCA accounts for more than 70% of the liquid and does not affect the general conclusions of the argument presented above.

Because of the complications described above, the historical source term for the organic liquids can only be roughly approximated. The major long-term source for organic contamination in the disposal shafts is expected to be from potential future releases as a result of drum deterioration.

3.2.3 Pore-gas monitoring network

Quarterly pore-gas monitoring has been conducted at the site since 1985 in accordance with a compliance ordered issued by the state of New Mexico [LANL, 2000]. Since 1997, 24 operational boreholes (Figure 1) have been sampled using a Bruel and Kjaer (B&K) Multigas Analyzer, Model 1302. The sample ports are purged until CO_2 concetration stabilizes, after which time five analytes (1,1,1-TCA, TCE, PCE, Freon, and CO_2) are measured. The B&K field screening data have been verified against laboratory analysis using SUMMA canisters and show consistent results. More details on the methodology can be found in LANL (2002).

Figure 4 shows the second quarter FY99 monitoring data of measured 1,1,1-TCA concentration at a depth of 18.3 m (60 ft.) below the mesa top contoured in map view. The data have been clipped at 10 ppmv to represent the lower limit of data reliability, which was reported as 5 to 10 ppmv. The spatial distribution of the waste leads to two main source regions for organic vapors, causing the development of the double-lobed plume seen in the site data. The major vapor-phase contaminant measured in the second quarter of FY99 was 1,1,1-TCA, which composed approximately 75% by volume of the spatially averaged plume. Continued monitoring of soil gas has shown that the organic vapor-plume source region is coincident with the disposal shafts, and that

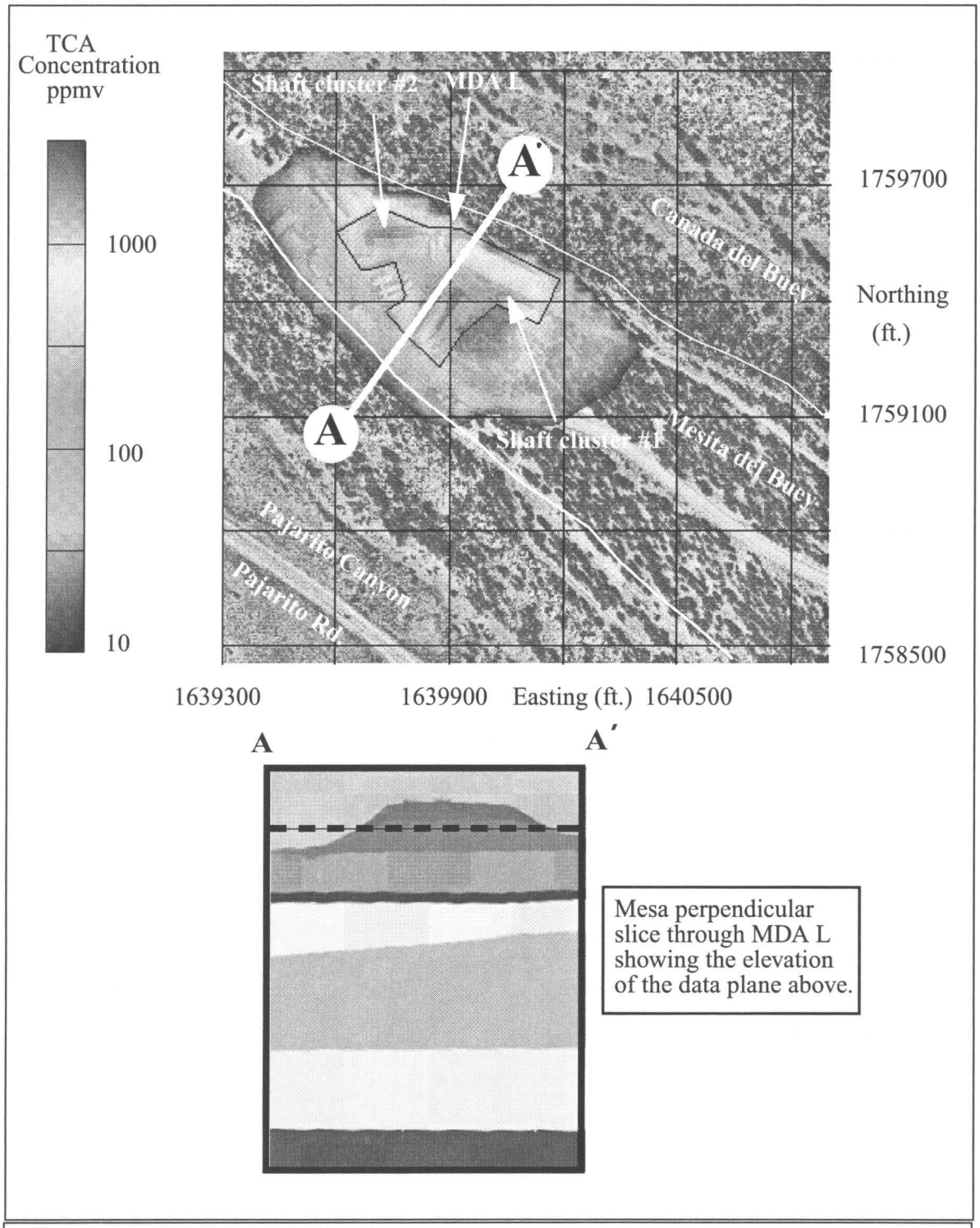

Figure 4 Second Quarter FY99, MDA L, TCA concentration data (log-scale) contoured on a plane 18 m below the mesa top.

the plume does not appear to have grown at a detectable rate over the period of 1997 through 1999 [Smith et al., 1998, 1999a, 1999b].

4.0 - Conceptual model, assumptions, and parameters

The conceptual model on which the numerical simulations are based contains several key features including saturation dependent vapor diffusion, Henry's Law partitioning, topographic boundaries in contact with the atmosphere, asphalt covering part of the site, and reduction in diffusion across the land/air interface due to boundary layer processes that may impede mass transfer. Diffusive behavior is assumed to be the fundamental mechanism controlling the migration of VOCs at the site. The effective vapor diffusion coefficient, D*(sat), accounts for both vapor diffusion and diffusive spreading induced by barometric pumping (Auer et al., 1996; Neeper, 2002). VOCs diffuse from the pore gas into the atmosphere along the mesa top and sides. This atmospheric boundary maintains a steep concentration gradient between the subsurface plume and the atmosphere so that the diffusive flux is greater toward the mesa top and sides and lower along the axis of the mesa and downward. More details and justifications for use of parameters in the conceptual model can be found in Stauffer et al. (2004).

Table 1: Physiochemical Parameters of 1,1,1-TCA (Little, 1987).

1,1,1-TCA ($C_2H_3CL_3$)	
Molecular weight	133 g/mol (at 293 K)
Liquid density	1325 kg/m3 (at 293 K)
Vapor pressure	100 mmHg (at 293 K) = 13.16 kPa
Water solubility (mg/l)	950 mg/L (at 293 K)
Tuff sorption coefficient Ong and Lions (1991)	< 0.5 mL/g
Henry's Law constant Jury (1990)	1.46 (dimensionless) C_{vapor}/C_{water}

4.1 Hydrologic properties

For this study, we use the same hydrologic and transport properties of Stauffer et al. (2004) which are repeated here in Table 2 .

Table 2: Physical Parameters used in the best-fit simulation

Unit	Effective porosity	In-situ saturation	Effective vapor diffusion coefficient D* (m^2/s)
Qbt 2	0.48	0.06	$4x10^{-6}$
Qbt 1 v	0.53	0.15	$2x10^{-6}$
Qbt 1 g	0.51	0.15	$2x10^{-6}$
Cerro Toledo	0.47	0.40	$0.4x10^{-6}$
Otowi Member	0.47	0.35	$0.4x10^{-6}$
Cerros del Rio basalt (matrix)	0.1	0.02	$4x10^{-6}$
Puye Formation	0.2	0.02	$4x10^{-6}$
Shafts	0.5	0.02	$4x10^{-6}$
Asphalt	0.5	0.02	$1x10^{-14}$
Surface (not including asphalt)	0.48	0.02	$1x10^{-6}$

4.2 TCA release

The migration of TCA vapor from the barrels in the shafts for the best-fit simulation of Stauffer et al. (2004) was conceptualized as a time-release phenomenon. This is based on the idea that liquid will leak slowly and quickly volatilize. The data from Lyons et al. (1996) support this conceptual model because the predominant mechanism for failure in the first 30 years of drum emplacement is caused by pinhole pitting failure. For this study, we assume that the pitting failure mode should lead to slow leaking, while the general structural failure of the drums is assumed to lead to catastrophic release of liquid TCA into the waste shafts.

Sudden increases in source strength are possible if individual drums of concentrated solvent burst, and drum corrosion data suggest this process to become more important from 30 to

70 years after emplacement [Lyon et al., 1996]. Thus, for this study, we have taken the best-fit model as a starting point in the year 2000 and examine the consequences of from 1 to 25 drums simultaneously failing with each drum releasing 281 kg of pure TCA into the system.

Non-aqueous phase liquids such as TCA that are virtually immiscible in water are expected to behave differently than water in the subsurface [Hayden et al., 1997]. Because these chemicals do not initially wet the surface of the rocks, and because of different surface tension and density, they have different capillary pressure/permeability curves that can lead to greater subsurface transport than one would expect for water [Dicarlo et al., 2000; Blunt et al., 1995]. For example, a 50,000-gallon tank of diesel fuel that leaked into the mesa at TA-21 has propagated to a depth of 140 ft below ground surface in less than 10 years [Haagenstad et al., 2002]. Although the source volume at TA-21 is significantly higher than the maximum drum failure scenario in this study (25 drums = 1375 gallons), the TA-21 data provide a maximum likely depth of migration for liquid-phase TCA in Bandelier Tuff.

Liquid-phase transport is not explicitly included in the physics of the simulations presented, however the TA-21 diesel fuel spill data are used to guide the modeling. In all simulations of catastrophic drum failure, the liquid TCA is conceptualized as having flowed into a pool at the bottom of the shafts (60 ft), and from there flowed rapidly downward distributing evenly to residual saturations between 60 ft and 140 ft below ground surface.

5.0 - Numerical model

The MDA L site model is a three-dimensional representation of the simplified subsurface stratigraphy including the surface topography. The numerical modeling is limited to diffusive transport of TCA vapor in the subsurface and reduces the complexity of the problem by neglecting advective transport of water, air, and VOC. Details of the numerical model and model domain can be found in Stauffer et al. (2004). Figure 5 shows a cross-section through the model domain with the geologic units labeled. This figure also shows the location of the water table.

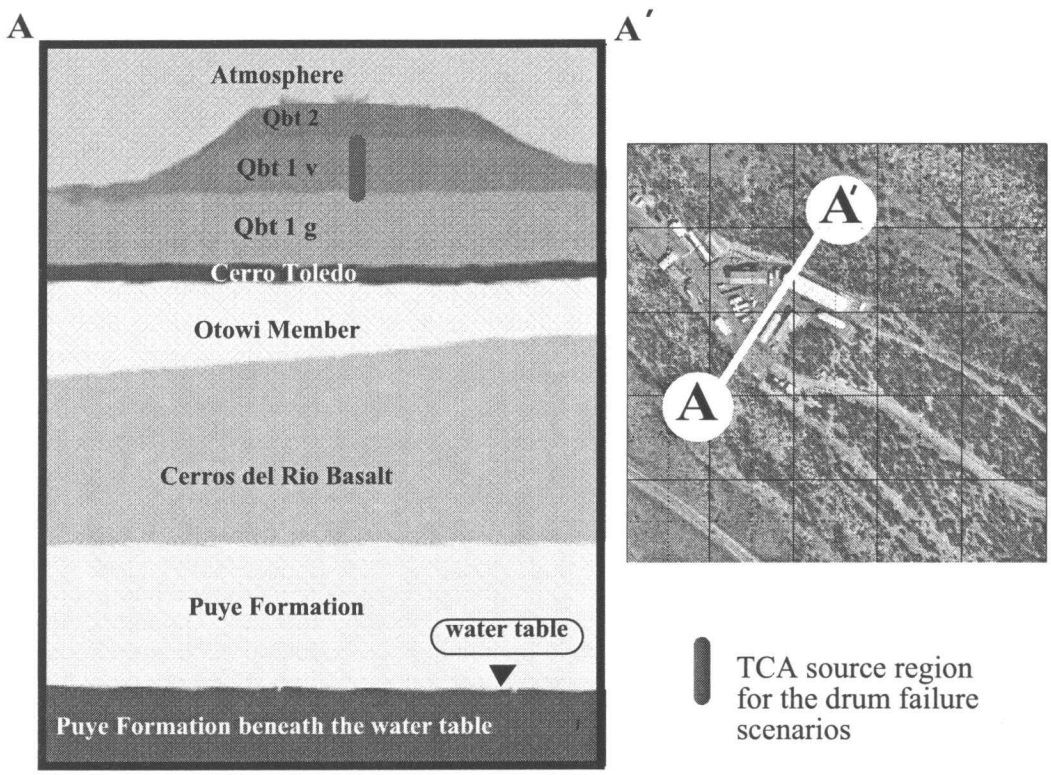

Figure 5 Model stratigraphy on cross-section A-A'

5.1 Boundary and initial conditions

The bottom boundary of the domain is flat and lies below the water table. No flow of water or vapor is permitted across the bottom boundary, and its temperature is held constant at 25°C, based on well bore measurements [Griggs, 1955]. The atmosphere at the top of the model is held at a pressure of 0.078 MPa (585 mm/Hg), and the temperature is fixed to the yearly average of 10°C [LANL weather website]. The atmosphere is represented by fixing the concentration at zero in the nodes above the land surface. The vertical side boundaries of the domain are no flow with respect to both mass and heat.

The soil-gas data were used in Stauffer et al. (2004) to calibrate a site scale numerical model that is able to recreate the distribution and magnitude of the measured plume at the year 2000. All drum failure calculations presented in this study begin from the best-fit calibrated model in the year 2000.

5.2 Hydrologic parameters

Hydrologic parameters used in the simulations are listed in Table 2 and discussed in more detail in Stauffer et al. (2004).

5.3 Shafts and asphalt

The model node spacing is too coarse to explicitly include each shaft found at MDA L. Therefore, we group the shafts into two clusters, with cluster #1 containing shafts 1 through 28 and cluster #2 containing shafts 29 through 34. Each cluster is specified using three nodes that include a volume of the model domain (3520 m^3) extending from two meters below the surface to a depth of approximately 20 meters. The model shafts coincide spatially with the two actual shaft clusters shown in Figure 3. The shaft nodes are assigned fixed concentrations of TCA based on the highest measured concentrations from vapor ports near the shafts.

The asphalt cover is modeled as having been laid down as one layer at the beginning of 1985. The timing of the asphalt cover is not well documented, and our approach is meant to capture the gross system behavior. In addition to the extensive asphalt covering within the boundaries of the site, substantial portions of the mesa around MDA L have been paved for parking lots, trailer foundations, and roads. The modeling presented below includes only the asphalt within the boundaries of MDA L.

The best-fit simulation of Stauffer et al. (2004) is based on slow leaking from the two shaft clusters from 1975 to the year 2000.

5.4 Drum Failure Considerations

This study extends the best-fit simulation (including the estimates of slow leaking) into the future with the addition of drum failure causing large inputs of TCA to be released beneath the two source regions. Thus, the simulations use the same fixed concentrations in the source region from

the best-fit calibration (as if slowly leaking drums were present) while at the same time injecting a pulse of TCA beneath the shafts to represent the drum failures.

Using the TA-21 diesel leak as a guide, we fix nodes below the shafts from approximately 60 ft to 140 ft at higher concentrations for varying amounts of time. The source region for the simulations of catastrophic failure is shown in red on Figure 5 and reaches from the base of unit Qbt 2 into the top of unit Qbt 1g. Each simulation requires the fixed concentration and length of time that this concentration is fixed to be adjusted to achieve the desired amount of input TCA. For example, simulation of a single drum failure using this conceptual model requires that the region below the shafts be fixed for 10 days at a concentration of 20,000 ppmv. For a 10 drum failure scenario, the sub-shaft region was again fixed for 10 days but at a concentration of very close to the vapor pressure limit of 160,000 ppmv. For 25 drums, the concentration was set at the maximum of 160,000 ppmv and was fixed for 357 days to generate a pulse of the required magnitude (7000 kg of TCA). Although the fixed values at the source are fairly arbitrary, they are constrained at the upper end by the vapor pressure of TCA, while the length of time for which these concentrations are fixed is constrained by the total mass necessary to create a vapor phase pulse containing the required number of 55 gallon drums.

6.0 - Results and Discussion

One main goal of this work is to show how catastrophic drum failure might be detected with the current monitoring boreholes. For this purpose, seven boreholes surrounding the site were chosen (54-1015, 54-1016, 54-2002, 54-2022, 54-2025, 54-2031, and 54-2087) to represent a possible early warning network. Simulated concentrations from these boreholes are used to demonstrate that such an early warning network could be used to trigger corrective actions if evidence for catastrophic release is detected. Boreholes 54-1015 and 1016, which extend into the Cerros Del Rio basalt, are included to give an estimate of the vertical growth of the plume. Because there are many sampling ports in each of these boreholes, the borehole ID is followed by the depth of the port in parentheses. For example the sampling port at 350 ft deep in borehole 54-1015 is refered to as 1015(350). The larger eastern shaft cluster (#1) was simulated with 1, 5, 10 and 25 simultaneous drum failures while the western cluster (#2) was simulated with 5 and 10 failures. Although many permutations of such failures can be envisioned, these end-members comprise a useful subset that demonstrates what changes may be seen in the monitoring wells that surround the site. To simplify the presentation of the results, all graphs of TCA concentration versus time are shown as increases above the best-fit simulation through time. First, the best-fit simulation was run to the year 2030, then the TCA concentration versus time was subtracted from each of the drum failure scenarios. This technique is useful because changes from the expected slow growth of the plume are what will signal catastrophic failure, and the simulations help to show where clearly measurable changes are most likely to be seen. Color contours on vertical and horizontal planes are shown in absolute concentration with contour lines labeled.

6.1 Catastrophic Drum Failure Beneath Shaft Cluster #1

Figure 6 shows the concentration of TCA above the best-fit case for both 1 drum (280 kg TCA) and 5 drums (1400 kg TCA) failing catastrophically in shaft cluster #1. The most heavily impacted sampling ports are found in boreholes 54-2087 and 54-2002. This result is quite reasonable because these are the two closest boreholes to the release site. The simulations show that concentrations in borehole is 54-2025, located approximately 150 ft to the east of the site, may have clearly measurable changes (50 ppmv) within 5-10 years.

Interestingly, the 1 and 5 drum failure scenarios appear to scale with the maximum concentration. Increased TCA arrives at nearly the same time for the set of ports shown in Figure 6, although the concentrations for the 5 drum case are about a factor of 5 greater than for the 1 drum

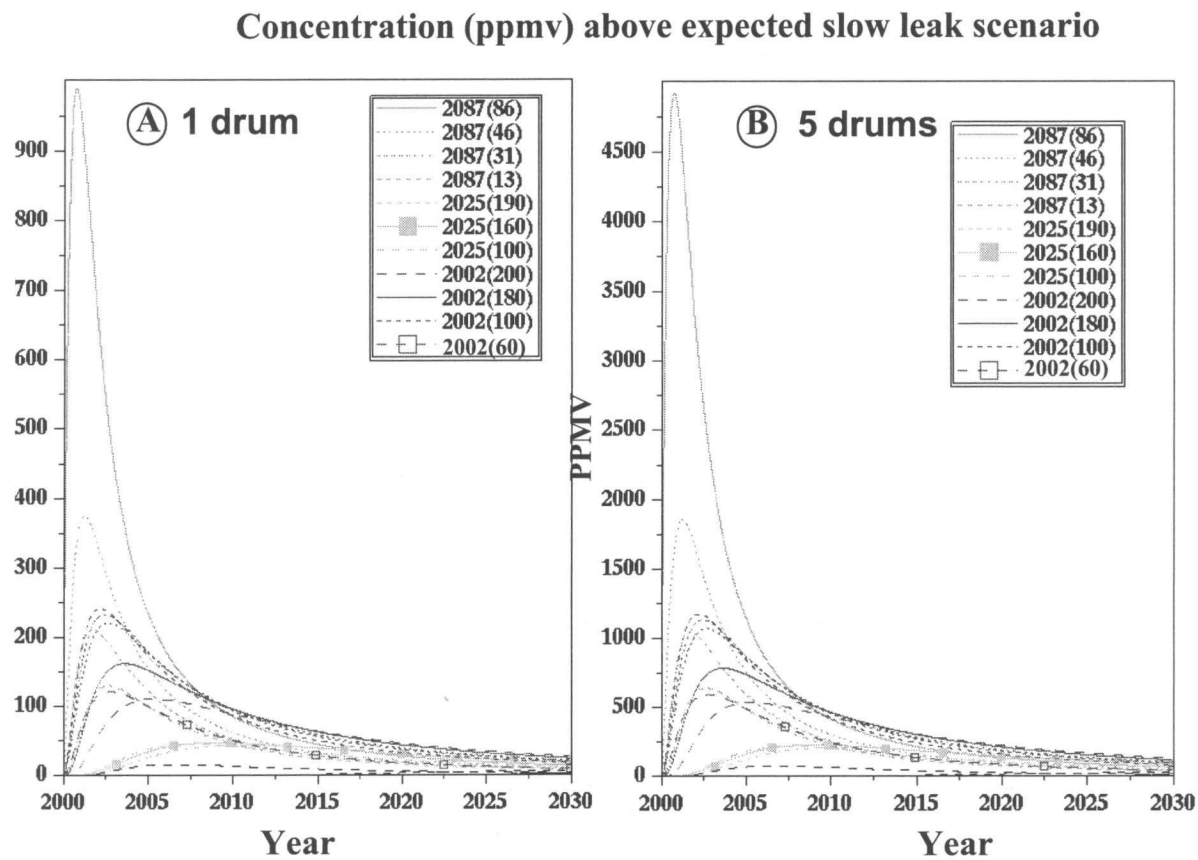

Figure 6 Simulated change in concentration of TCA for a single 55 gallon drum failure (A) and 5 drums failing (B) beneath shaft cluster #1.

case. Results for 10 drums (2800 kg TCA) scale likewise and have a maximum concentration at 2087(86) of almost 10,000 ppmv.

The results for 25 drums (7000 kg TCA) failing simultaneously in shaft cluster #1 also scale quite well with a maximum in 2087(86) of 22,600 ppmv. Figure 7 shows the results for the 25 drum scenario with a close-up of the lower 500 ppmv. The close-up shows that there would probably be measurable concentration increases in surrounding boreholes that are less impacted by the smaller releases. The furthest point that is clearly impacted is 2031(100), approximately 400 ft from the release, which shows a steady increase to more than 50 ppmv from 2010 through 2030. At about the same time, the model predicts that data location 1016(318), located directly below the site in the Otowi member, would begin a steady rise and show a clearly measurable increase of over 200 ppmv by the year 2030. The model also predicts that the top of the basalt below the site (well 1016(390)) could show an increase of 100. ppmv while the simulation predicts only 10 ppmv for the deepest port 1016(601). Predictions for year 2030 TCA concentrations in the basalt in borehole 1015 are much lower with values very near 5 ppmv.

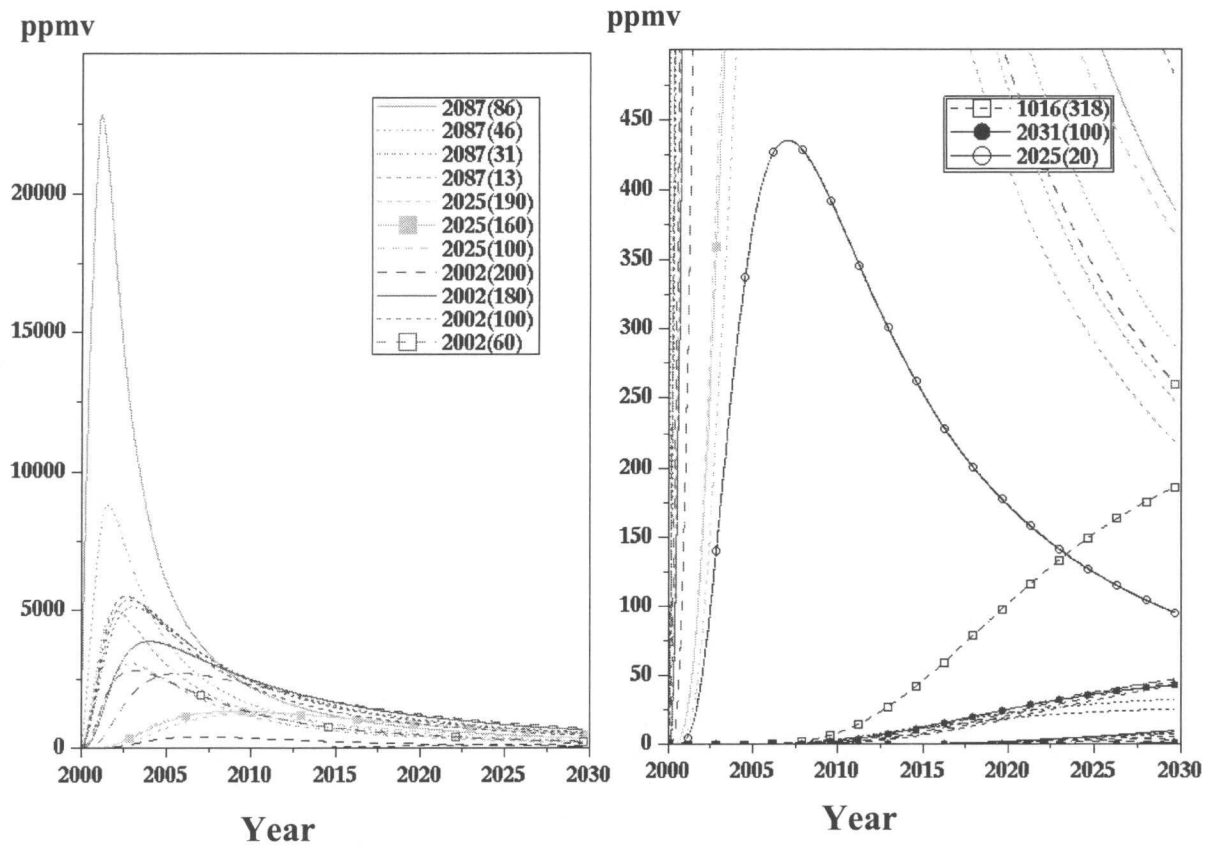

Figure 7 Simulated change in concentration of TCA for 25 drums failing beneath shaft cluster #1. The right figure is a blow-up of the lower 500 ppmv and shows that distant boreholes would likely be impacted by such a large impulse of TCA.

Figure 8 shows TCA concentrations on a plane 160 ft below the mesa top for the 25 drum failure case in the simulated Year 2001 at which time the entire 7000 kg of TCA have been introduced to the domain below the eastern shaft cluster (Cluster #1). The simulated plume at this depth has a maximum TCA concentration of greater than 30,000 ppmv.

6.1.1 Predicted shape of the plume in 2030

Predictions for how the TCA plume will grow by the year 2030 for cross-section A-A' are shown on Figure 9 for the best-fit case with continued slow leaking due to pinhole failures and for both the 10 drum and 25 drum catastrophic release scenarios in shaft cluster #1. As more TCA mass is added to simulate drum failure, the plume in the year 2030 grows both laterally and vertical. Figure 10 shows a horizontal plane at elevation 6640 ft (about 160 ft below the surface) with TCA contours for the same three cases.

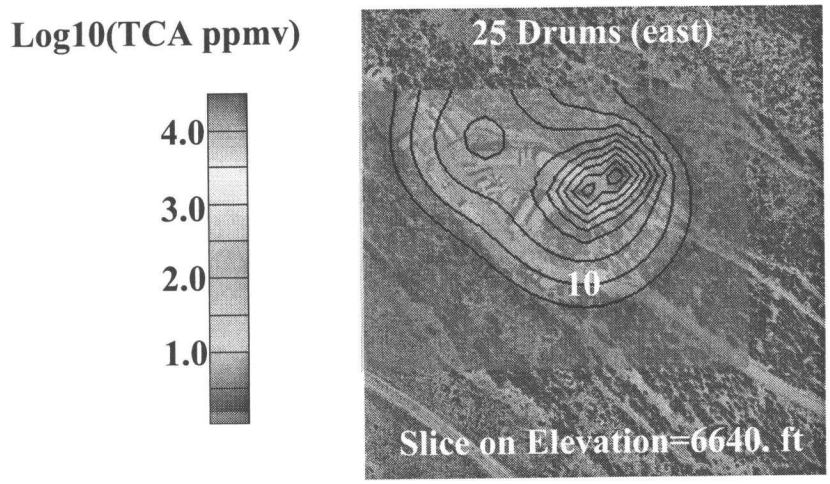

Figure 8 Simulated plume on a slice at elevation 6640 ft for the year 2001. Contours are in log-scale every half-order of magnitude with 10 ppmv labeled.

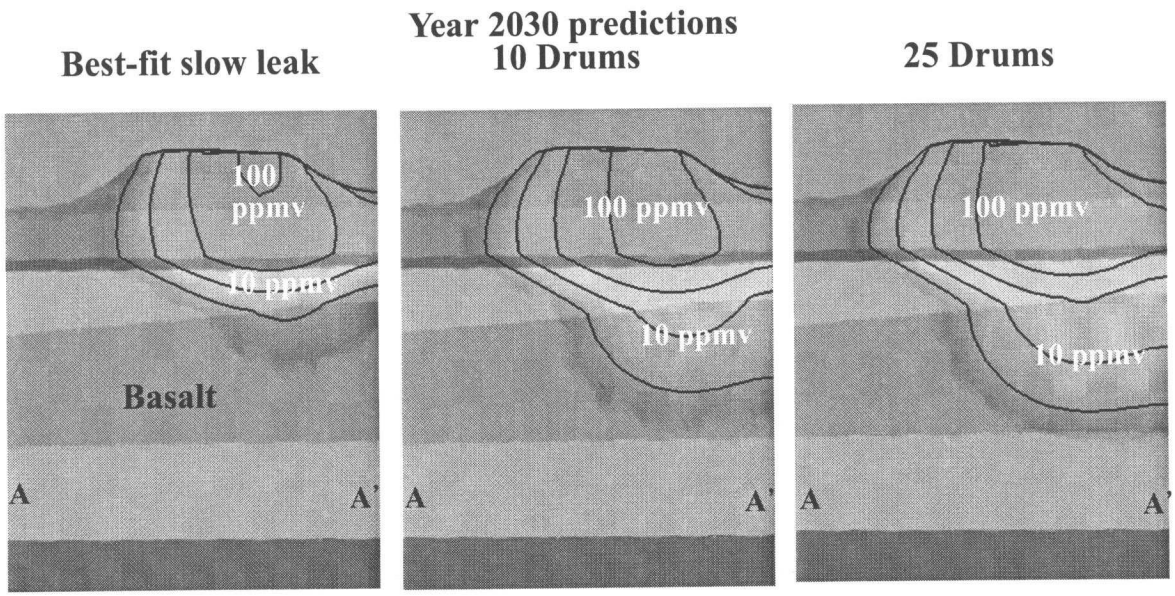

Figure 9 Simulated plume on cross-section A-A' for the year 2030. Contours are in log-scale every half-order of magnitude. Plume color-bar is the same as shown on Figure 8

6.2 Catastrophic Drum Failure Beneath Shaft Cluster #2

Drum failure in the western shaft cluster (Cluster #2 shown on Figure 4) impacts vapor concentration in a different set of boreholes, ones located closer to that source region. Figure 11 shows the simulated increase in TCA concentration at selected sampling ports for the 5 and 10 drum failure scenarios beneath shaft cluster #2. The results scale almost exactly with the total mass of TCA introduced during the catastrophic failure, with the maximum increase above background

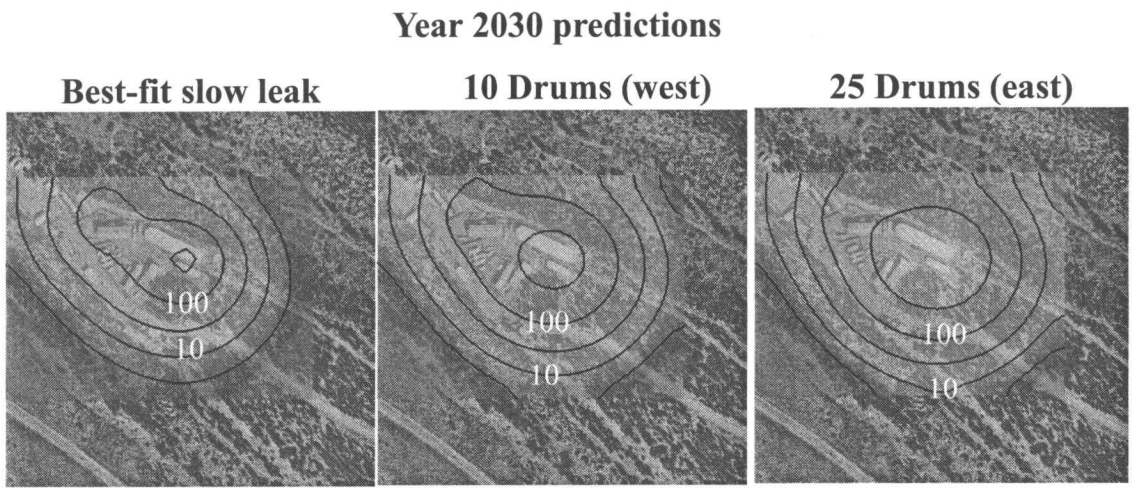

Figure 10 Simulated plume a slice at elevation 6640 ft for the year 2030. Contours are in log-scale every half-order of magnitude. Plume color-bar is the same as shown on Figure 8

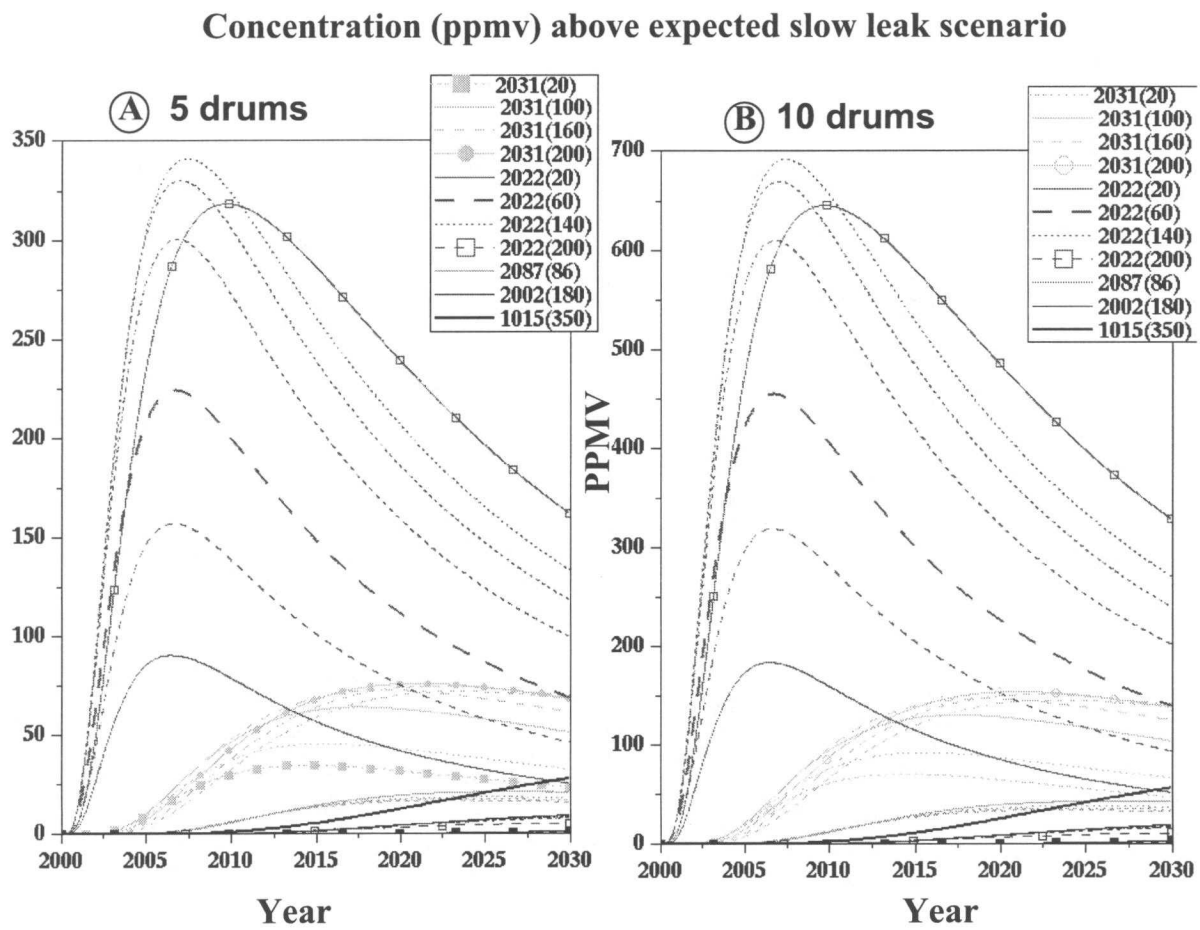

Figure 9 Simulated change in concentration of TCA for 5 drum failures (A) and 10 drums failing (B) beneath shaft cluster #2 on the western edge of the site.

doubling from near 350 ppmv for the 5 drum scenario to near 700 ppmv for the 10 drum scenario. As expected, the most heavily impacted sampling ports are located closer to the location of the release. Borehole 54-2022 has the strongest signal and would show a clear indication of catastrophic failure within 2-3 years. Borehole 54-2031 would show a measurable increase. However this signal takes more than 5 years to reach the sampling ports and does not peak until approximately 20 years after the release. Sampling port 1015(350), which lies nearly directly below the simulated release location, shows a measurable increase at times greater than 20 years after the release. Because of the quick response seen in Borehole 54-2022 as compared to the other holes in our hypothetical early warning network, we conclude that boreholes located at this distance from the source regions are ideally situated to give an early warning that catastrophic faliure has occured and such warnings would allow time to implement a venting strategy.

6.3 Conservative Assumptions

Several conservative assumptions have been used in the simulations that lead to a plume that is larger than we may realistically expect.

6.3.1 Boundary Effects

A major assumption is that the boundaries of the model do not impact the growth of the simulated plumes. The model boundary is, however, impacting the solution for all three cases (Figures 10 and 11) In particular, for the 25 drum case the impact is much larger with the 100 ppmv contour line touching the model boundary. Boundary effects will cause the simulated plume to push deeper into the subsurface than if the simulations were run with the lateral boundaries moved farther from the source region. It is evident that although the impacts of boundary effects may be relatively minor for the best-fit case, simulations with large numbers of drum failures (10+) should use a numerical grid that is larger to allow the simulated plumes to spread laterally. Increased lateral spreading will provide the additional benefit of providing more atmospheric interaction allowing more of the simulated plume to vent.

6.3.2 Basalt

Another conservative assumption in the simulations with respect to vertical transport toward the water-table is that the basalt is treated as a homogeneous low porosity material. Site data show that although the basalt lies well below the ground surface, measurements of pressure in this unit from boreholes 54-1015 and 54-1016 are in-phase with the atmosphere and nearly the same magnitude (Neeper, 2002). This implies that the basalt is well connected to outcrop which lies in

the direction of White Rock, on the order of 3 km toward the southeast. Furthermore, pressure data presented in Neeper (2002) show conclusively that the basalt is well connected on the scale of hundreds of meters with very high transmissivity.

The Neeper (2002) data suggest that passive venting in the basalt, The high connectivity in the basalt provide an excellent opportunity for passive venting if a network of boreholes were drilled around the site. could provide an easy way to remove vapor-phase contaminants from beneath MDA L. Another profound implication of such venting would be increased evaporation that would effectively reduce any liquid-phase transport through the basalt located beneath TA-54. Increased evaporation would result from atmospheric air that has less than 100% humidity interacting with soil gas that is generally at 100% humidity. Modeling of such a system will be used in the Corrective Measures Study (CMS) to evaluate design parameters and optimize the ability of a limited number of boreholes to remove TCA vapor and water vapor from the subsurface.

6.3.3 Asphalt and Surface Changes

The final conservative assumption in these calculations is that the surface remains in its current condition with asphalt as a diffusive barrier for the entire 30 years of simulated time. Because the asphalt is limiting the transport of TCA along the shortest pathway to the atmosphere, this assumption causes the large input during drum failure to spread more laterally and vertically than if the asphalt were removed at some point during the next 30 years. Site remediation expected to be completed by 2010 will include removal of the asphalt and installation of a vegetated landfill cover. Additionally, the CMS may recommend installation of a passive venting network that would facilitate removal of TCA vapor from the subsurface. These remediation steps will allow the plume to vent more easily to the surface and would dramatically alter the long term growth of the plume. Simulations of venting scenarios in the CMS will include removal of the asphalt.

7.0 - CONCLUSIONS

Simulations of catastrophic drum failure at MDA L demonstrate that the current pore-gas monitoring network would show clear evidence of such failure and allow sufficient time to implement corrective measures to mitigate possible impacts to the environment. Although several conservative assumptions were used in the conceptual model, the results are robust and yield insight into the probable behavior of catastrophic releases at this site for evaluation in the Corrective Measures Study.

Because any sudden release from the site must propagate outward from the source region, the most logical sentry wells for such an event are the boreholes closest to the source region. One reasonable approach to the pore-gas monitoring at this site would be to reduce the frequency of monitoring at outlying boreholes while maintaining a more frequent sampling program at a set of wells that are within a 100 ft radius of the source region. This approach would be more cost effective than the current sampling program while providing the same level of protection.

These simulations highlight the need to better understand the probable nature of drum failure over the next few decades as well as underscoring the need to more accurately characterize the composition and configuration of waste in the shafts at MDA L.

8.0 - Acknowledgements

We would like to thank Kay Birdsell and Ken Kisiel for thier helpful reviews of this document.

9.0 - REFERENCES

Auer, L.A., N.D. Rosenberg, K.H. Birdsell, and E.M. Whitney, (1996). The Effects of Barometric Pumping on Contaminant Transport, J. Contaminant Hydrology (24), 145-166.

Blunt, M., D. Zhou, and D. Fenwick , (1995). Three-Phase Flow and Gravity Drainage in Porous Media, Transport in Porous Media, (20), 77-102.

Dicarlo, D.A., A. Sahni, and M. Blunt, (2000). The Effect of Wettability on Three-Phase Relative Permeability, Transport in Porous Media, (39), 347-366.

Fetter, C.W. (1999), "Contaminant Hydrogeology", Prentice-Hall, NJ, USA.

George, D. (1997). Unstructured Toolbox for Modeling and Simulation, LA-UR-97-3052, presented at the 1997 Workshop on Computational Electronics and Nanoelectronics, Urbana, Illinois, October 20-22, 1997.

Griggs, R.L. (1955). Geology and Groundwater Resources of the Los Alamos Area, New Mexico, U.S. Geologic Survey Report to the U.S. Atomic Energy Commission.

Haagenstad, M.P., F. Caporuscio, and P.H. Stauffer (2002) TA-21-57 Aboveground Storage Tank Diesel Fuel Oil Environmental Assessment and Characterization, Los Alamos National Laboratory Report LAUR-02-4007.

Jury, W.A., D. Russo, G. Streile, and H. Abd, (1990). "Evaluation of Volatilization by Organic Chemicals Residing Below the Soil Surface", Water Resources Research, 26(1) p. 13-20.

LANL (2000). "RFI Report for Material Disposal Areas G, H, and L at Technical Area 54," Los Alamos National Laboratory report LA-UR-00-1140.

LANL (2002). "RFI Report for Material Disposal Area L at Technical Area 54," Los Alamos National Laboratory report LA-UR-02-7803.

Little, A.D. (1987). The Installation Restortation Program Toxicology Guide, Vol. 1, 1-16.

Lyon, B.F., Holmes, J.A., Kosiewicz, S.T., Wilbert, K.A., Travis, C.C. (1996). Estimation of corrosion on carbon steel TRU waste drums using Poisson distribution, J. Hazardous Materials, 51, p. 165-179.

Neeper, D.A. (2002). Investigation of the vadose zone using barometric pressure cycles, J. Contaminant Hydrology (54), 59-80.

Purtymun, W.D., (1995). "Geologic and Hydrologic Records of Observation Wells, Test Holes, Test Wells, Supply Wells, Springs, and Surface Water Stations in the Los Alamos Area," Los Alamos National Laboratory manuscript LA-12883-MS.

Reneau, S.L., D.E. Broxton, J.S. Carney, and C. LaDelfe (1998), Structure of the Tshirege Member of the Bandelier Tuff at Mesita del Buey, Technical Area 54, Los Alamos National Laboratory, Los Alamos National Laboratory manuscript LA-13538-MS

Smith, R.L. and Bailey, R.A. (1966). "The Bandelier Tuff: A Study of Ash-Flow Eruption Cycles and Zoned Magma Chambers," Bulletin of Volcanology 29, 83-104.

Smith, J., Hardesty, B., McCranie, N. (1999a), Quarterly Pore Gas Sampling at TA-54 MDA L and MDA G First Quarter FY1999, PMC-LA-99-002.

Smith, J., Hardesty, B., McCranie, N. (1999b), Quarterly Pore Gas Sampling at TA-54 MDA L and MDA G Second Quarter FY1999, PMC-LA-99-003.

Smith, J., Crocker, J., McCranie, N. (1998), Quarterly Pore Gas Sampling at TA-54 MDA L and MDA G Second Quarter FY1998, PMC-LA-98-009.

Stauffer, P.H., K.H. Birdsell, M.S. Witkowski, and J. Hopkins (2004). Vapor-Phase Transport of within a Mesa: Conceptual Model Validation through Numerical Simulation, submitted to Vadose Zone Journal.

Vaniman, D., G. Cole, J. Gardner, J. Conaway, D. Broxton, S. Reneau, M. Rice, G. WoldeGabriel, J. Blossom, and F. Goff, (1998). "Development of a Site-Wide Geologic Model for Los Alamos National Laboratory," Los Alamos National Laboratory unpublished document.

List of Tables

1. Physiochemical Properties of 1,1,1-TCA
2. Physical parameters used in the best-fit simulation

List of Figures

1. Geographical information for MDA L and the surrounding area.
2. Simplified site stratigraphy.
3. Location map for waste disposal shafts and pits at MDA L
4. Second Quarter FY99, MDA L, TCA concentration data (log-scale) contoured on a plane 18 m below the mesa top.
5. Model stratigraphy on cross-section A-A'
6. Simulated change in concentration of TCA for a single 55 gallon drum failure (A) and 5 drums failing (B) beneath shaft cluster #1.
7. Simulated change in concentration of TCA for 25 drums failing beneath shaft cluster #1.
8. Simulated plume on a slice at elevation 6640 ft for the year 2030.
9. Simulated change in concentration of TCA for 5 drum failures (A) and 10 drums failing (B) beneath shaft cluster #2 on the western edge of the site.
10. Simulated plume on cross-section A-A for the year 2030.
11. Simulated plume a slice at elevation 6640 ft for the year 2030.